Iraqi Journal of Science, 2017, Vol. 58, No.2B, pp: 920-928
DOI:10.24996.ijs.2017.58.2B.16

ISSN: 0067-2904

Iris Outer Boundary Localization Based on Leading Edge Technique

Ahmed H. Adil[*1], Ayad A. Abdul-Salam[2]
[1] Department of Computer Science, College of Science, University of Baghdad, Baghdad, Iraq.
[2] Department of Computer Science, College of Education for Women, University of Baghdad, Baghdad, Iraq.

Abstract

In recent years, the iris biometric occupies a wide interesting when talking about biometric based systems, because it is one of the most accurate biometrics to prove users identities, thus it is providing high security for concerned systems. This research article is showing up an efficient method to detect the outer boundary of the iris, using a new form of leading edge detection technique. This technique is very useful to isolate two regions that have convergent intensity levels in gray scale images, which represents the main issue of iris isolation, because it is difficult to find the border that can separate between the lighter gray background (sclera) and light gray foreground (iris texture). The proposed method tried to find iris radius by seeking in the two iris halves (right and left) circularly, in term of certain angles interval for each half, to avoid the existence of the upper and lower eyelids and eyelashes. After the two radiuses (i.e. for each half) had been determined, the iris final iris radius would be evaluated to the minimum value of them. This method tested on all samples of CASIAv4-Interval dataset, which consist of 2639 samples, captured from 249 individuals, and distributed on 395 classes, the accuracy of the testing was 100% for outer boundary detection.

Keywords: Iris Biometric, Iris outer boundary, Iris segmentation, Leading edge technique, Convergent intensities isolation.

إستكشاف الحدود الخارجية لقزحية العين بالإعتماد على تقنية الخط الموجّه

أحمد حسن عادل*[1]، أياد عبد القهار عبد السلام[2]
[1]قسم الحاسبات، كلية العلوم، جامعة بغداد، بغداد، العراق.
[2]قسم الحاسبات، كلية التربية للبنات، جامعة بغداد، بغداد، العراق.

الخلاصة

أخذت قزحية العين جانب كبير من الأبحاث المختصة بأنظمة تمييز الأشخاص عن طريق الصفات البيومترية في السنوات الأخيرة، نظراً لما تتمتع به هذه الصفة من دقة عالية في التمييز واثبات هوية المستخدمين، وبالتالي توفير أمان عالي للأنظمة المعنية. هذه المقالة البحثية تستعرض طريقة كفوءة لاستكشاف الحدود الخارجية للقزحية، باستخدام شكل جديد لتقنية الخط الموجّه. هذه التقنية مساعدة جداً لعزل منطقتين لها مستويات متقاربة من التدرجات الرمادية في الصور الغير ملونة، وهو ما يمثل أحد مشاكل عملية عزل قزحية العين، لأنه من الصعب إيجاد الحدود الفاصلة بين خلفية الصورة ذات اللون الرمادي الأفتح (بياض العين) والأجسام الواقعة عليها ذات اللون الرمادي الفاتح (نقشة القزحية). الطريقة المقترحة تحاول

*Email: corazon.compunet@gmail.com

إيجاد نصف قطر القزحية بالبحث في جانبيها الأيمن والأيسر بشكل دائري، وضمن حدود فترة معينة من الزوايا لتجنب وجود الجفون والرموش العليا والسفلى. بعد ان يتم تحديد نصف القطر في كلا الجانبين، يتم اعتماد نصف القطر النهائي عن طريق إيجاد نصف القطر الأقل بينهما. هذه الطريقة تم إختبارها بإستخدام كل عينات قاعدة بيانات CASIAv4-Interval، والتي تحتوي على 2639 عينة مأخوذة من 249 شخص، وموزعة على 395 صنف، وكانت نسبة النجاح فيها 100% في إستكشاف الحدود الخارجية للقزحية.

Introduction

Iris biometric is respected to be the most reliable and accurate for biometric-based systems, since the iris texture pattern uniqueness is very high, in additional to its stability during individual lifetime. Therefore, iris-based identification systems keep growing in the modern technologies. Iris segmentation is the localization of both inner and outer boundaries of the colored ring of the eye [1]. The accurate iris isolation from its nearby undesired objects (e.g. pupillary area, sclera area, eyelids, and eyelashes) is the master issue of any iris recognition system [2], so that it must be found an accurate segmentation method to increase the opportunity of recognition and identification accuracy.
The individual iris is the area confined between pupillary region (inner boundary) and sclera region (outer boundary), which has a unique texture implementation. Furthermore, it can be acquired through certain distance, without need for physical contiguity, which make it desirable over other biometrics [3]. Iris segmentation is not ordinary task, because of the occlusion of eyelids and/or eyelash, poor contrast and brightness, pupillary dilation, etc. [4].

Iris pupil is designed in a way to control the quantity of passes to the retina of the human eye, its size varies according to the brightness of illumination, and therefore the pupil constricted and dilated [5], which causes unfixed texture area width. The proposed method tries to determine an accurate iris outer boundary (i.e. iris/sclera isolation) although the iris texture and sclera intensity levels are convergent in iris gray scale images.

Literature Review

Iris boundaries localization methods are many and different, but most of them based on iris localization classical methods. Examples of famous classical methods those which have been invited by *Daugman* [6] and *Wildes* [7]. Daugman's method computes the inner and outer boundary coordinates using integro-differential operator, by seeking in blurred partial derivative over the input image for maximum possible circle radius to localize both boundaries, while Wildes' method was based on edge detection using gradient-based method, then applying Circular Hough Transform (CHT) to localize both boundaries.

L. Ling and D. de Brito [8] proposed iris segmentation method. For iris localization, they cropped the image to a some region of interest then filtered the cropped image by median filter, and binarized the result by threshold value equal to the average of two gradient values that estimated by Sobel operators of median filtered image. Then determined a set of points belongs to iris boundary through Euclidian distance measure between each point to the pupil center, and suggested that iris center point is the midpoint of the points set and iris radius is the is the average of distances. *M. K. Mahadeo et al* [9] proposed a method to detect both boundaries by the use of same criteria, by computing the image convolution with certain filter using some convolution operator. The filter that used in this method was 1D Petrou-Kittler of smaller width for inner boundary localization and wider one for outer boundary detection.

A. A. Jarjes et al [10] are used a method for iris outer boundary detection based on Angular Integral Projection Function (AIPF) with a combination of Mahalanobis distances to estimate outer boundary points. *M. Mahlouji and A. Noruzi* [11] are used Canny Edge Detection (CED) image and CHT, by multiplying edge points matrix by constant value equal to 2.76 to estimate better edge of outer boundary, to be localized by CHT. *A. Basit et al* [12] computed iris outer boundary radius based on pupil center (that achieved by their proposed method for inner boundary) and two searching sectors (one for right side and the other for left side) to obtain the points with maximum change rate in the standard deviation. *R. Gupta and A. Kumar* [13] used K-mean clustering and vertical CED to find the iris region, and CHT to estimate the iris boundaries.

Initialization

The proposed method for inner boundary localization was based on some of digital image processing concepts; min-max contrast stretching, gamma correction, and seed (flood) filling technique. The method starts with determining the Region of Interest (RoI) surrounding the pupillary area, then tries to locate a pixel ($P_{x,\ y}$) inside pupil, which is assigned to the index of lowest gray intensity of the mean-filtered iris image. Thereafter, the specular spots reflected by capturing source is detected and filled using Gamma-based binarizer and seed filling technique, the filling task was done on the iris image instead of the binary image, to be appeared as full-darkest region of the iris image. Then the processed iris image is binarized using Gamma-based binarizer with different coefficients that used in specular spots detection.

At this point of processing, the binary image appears as foreground (black pupil and eyelashes) and white background. Closing morphology is applied on the binary image to reduce the eyelashes that may affect the accuracy of detection. The $P_{x,\ y}$ that is located inside pupillary area would be as a seed point for flood filling algorithm to collect the set of pupillary region points. The minimum and maximum x and y coordinates of the set assigned to be the most top-left and most bottom-right points of the pupil window, then the center of the pupil computed by mathematical mid-point of the mentioned two points. While the inner boundary radius computed through trigonometric functions to generate two initial elliptic radiuses. A simple detector was proposed to catch the thick eyelash-pupil connectivity to fit the inaccurate cases. The final iris radius computed after testing the detector condition, it is equal to the average of the two initial radiuses.

Proposed Method

Now, the pupil center C and pupil radius R_p is ready to be as input for outer boundary localization that passes through:

1. Filtering Iris Image Using Mean Filer

In order to make the isolation of iris/sclera more accurate, the averaging of levels of eye regions is useful. This process can be achieved by the use of mean filter of kernel 5×5 to be applied on the iris image. This step is found to restrict the effect of sharpness of iris texture edges. To reduce the filtering time, the mean filter would applied on a certain window surrounding the point C, let it of size 100×100 pixels.

2. Selecting the Seeking Regions

This stage depends on pupil coefficients (C, R_p) directly to determine two annular overlapped regions, so that the outer boundary of the iris does not exceed the mutual zone of the two proposed annular regions. The equations bellow describe selection of these regions:

$$A_{region} = \beta_{As} + R_p \dots \ \beta_{Ae} \quad (1)$$

$$B_{region} = \beta_{Bs} \dots \beta_{Be} \quad (2)$$

$$C_{regions(A\ and\ B)} = C \quad (3)$$

Where A_{region} and B_{region} is the two annular overlapped regions, Rp is pupil redius, $C_{regions(A\ and\ B)}$ is the center of regions A and B, C is the pupil center, and β_{As}, β_{Ae}, β_{Bs}, and β_{Be} are region A and B coefficients, so that to achieve overlapping, it must satisfy the condition ($\beta_{As} + R_p < \beta_{Bs} < \beta_{Ae} < \beta_{Be}$). These four coefficients are estimated by testing. The seeking process is circular, at both left and right halves, through angular interval from -10^o to 35^o for right half, and 145^o to 190^o for the left half. The Figure-1 describes the seeking region determination.

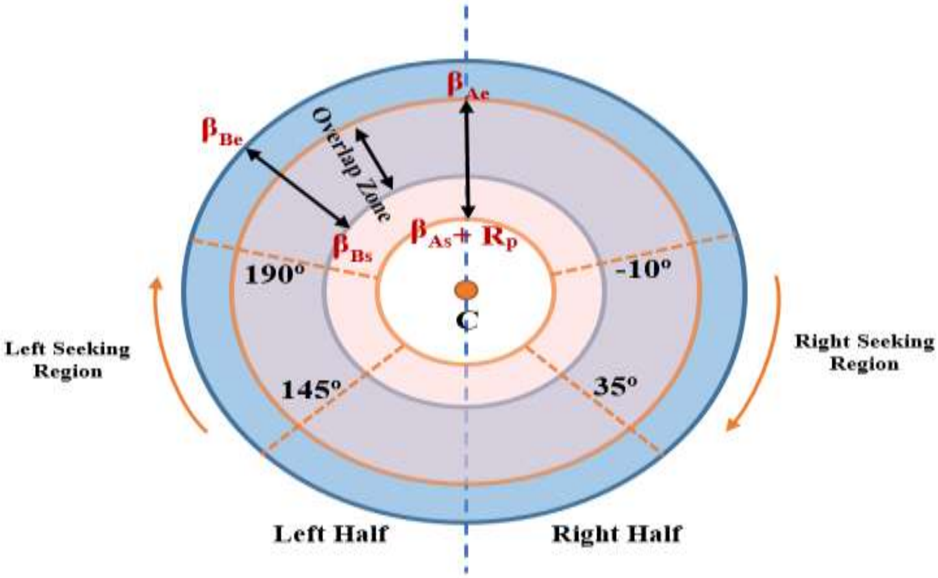

Figure 1 – Proposed Seeking Region.

3. Seeking Vectors (Leading Edges) Generation

After the selection of the seeking region, 23-vectors for each half (right and left), would be generated, (i.e. 46 vector in total), Figure-2. Each vector reflects a special case of leading edge. The values of each vector are streams of 0's and 1's, which are generated by a new form of leading edge technique, as the following sub steps:

a- Calculate the mean value of the points along the line at current angle direction θ (start by -10^o for right half, and by 145^o for the left half) from the low boundary of A_{region} to the high boundary of B_{region} (i.e. from $\beta_{As} + R_p$ to β_{Be}) so that:

$$\mu_\theta = \frac{1}{\beta_{Be}-\beta_{As}-R_p} \sum_{r=\beta_{As}+R_p}^{\beta_{Be}} I(r,\theta) \quad (4)$$

$$I(r,\theta) = I\big((C_x + r\cos\theta),(C_y + r\sin\theta)\big) \quad (5)$$

Where μ_θ is mean value of the points along the line at current angle θ, r is the current radius, $I(r, \theta)$ is the image value at index (r, θ).

b- Generate the vector of current θ by testing the points position and value, under the following circumstance:

$$V_\theta(i) = \begin{cases} 0, & I(r,\theta) \le \mu_\theta \text{ or } r < \beta_{Bs} \\ 1, & I(r,\theta) > \mu_\theta \text{ or } r > \beta_{Ae} \end{cases} \quad (6)$$

Where $V_\theta(i)$ is the i^{th} vector belongs to current θ.

c- Dispose the short breaks of 0's and 1's from current vector $V_\theta(i)$.

d- Increase θ by **two**

e- If θ ≤ (35 for right half, 190 for left half) Go to step (a) to assess the next vector, else **stop**.

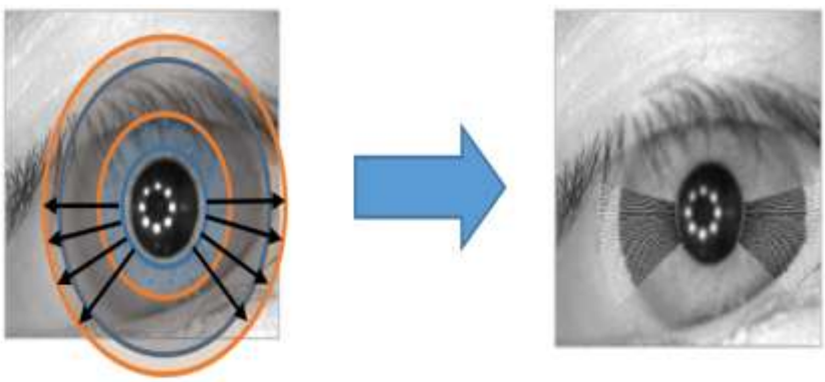

Figure 2 – Seeking Vectors Implementation

Algorithm (1) showing the process of leading edge vectors generation.

4. Estimating Iris Radius

Before finding iris radius and center point, a set of operations must applied to the vectors those generated in the previous step, these operations are:

a. Calculate the 1's stream length for each vector, rather than of 0's stream, because the 1's stream is clearer than 0's stream (it is included less 0's breaks than the 1's breaks of 0's stream).

b. Subtract the calculated length of 1's from the vector length to calculate the more accurate length of 0's stream.

c. Collect two sets of 0's lengths, for both left and right halves.

d. Ignore the lengths those are equal to ($\beta_{Ae} - R_p$) or equal to ($\beta_{Bs} - R_p$)

e. For each set compute three values, mean, median, and most frequent, to test the value that would give the accurate outer boundary radius

f. The final radius can be calculated through the following equations:

$$R_{right} = R_p + M_{s1} \quad (7)$$
$$R_{left} = R_p + M_{s2} \quad (8)$$
$$R_i = Min(R_{right}, R_{left}) \quad (9)$$

Where R_{left} and R_{right} are the left and right radiuses respectively, M_{s1} and M_{s2} are the represent the best value among mean, median, and most frequent values of the set1 (right half) and set2 (left half) respectively, R_i is the outer boundary (iris) radius. Figure-3 shows up the result of the proposed outer boundary localization. Algorithm (2) showing the process of computing iris radius.

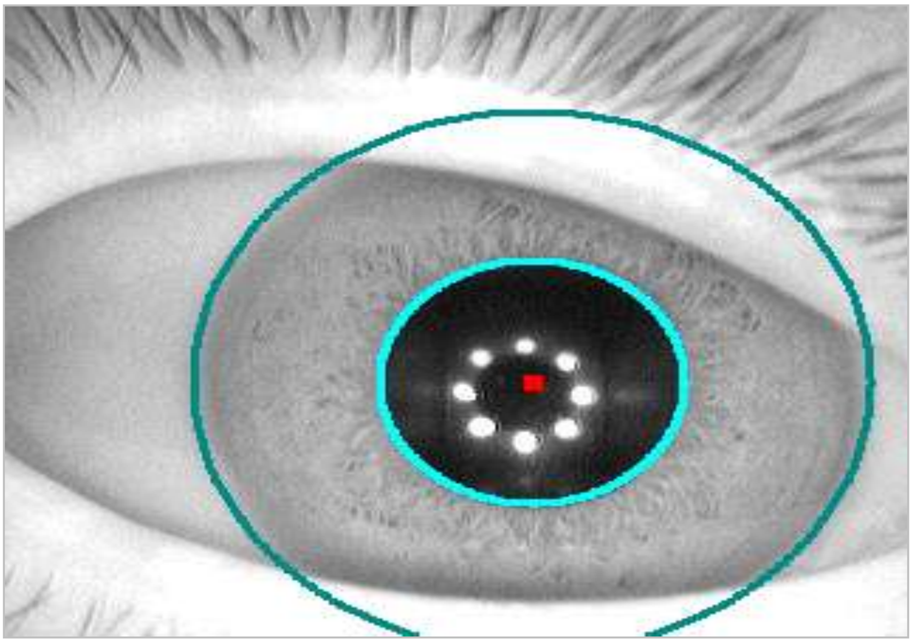

Figure 3– Proposed Iris Outer Boundary Localization

Algorithm 1- Leading Edge Vectors Generation		
Input	Img() w, h C, R_p BAs, BAe, BBs, BBe	*'Iris Image* *'Image width, height* *'Pupil Center Point, Radius Respectively* *'A Region Boundaries, B Region Boundaries*
Output	V	*'Seeking Vectors*

Processing	**Set** Ws ← 5
	Set MImg() ← **MeanFilter**(Img, w, h, Ws)
	Set Source ← BAs - R_p, Destination ← BBe - R_p, L ← Destination - Source
	Define V(46, L)
	Set i ← 0, j ← 0
	For all th **Do Step** 2{-10 ≤ th ≤ 34 or 146 ≤ th ≤ 190}
	Set Avg ← 0, Count ← 0
	For all r **Do** {Source ≤ r ≤ Destination}
	Set x ← C.x + (r * cos(th*pi/180))
	Set y ← C.y + (r * sin(th*pi/180))
	If x ≥ 0 **And** x ≤ w-1 **And** y ≥ 0 **And** y ≤ h-1
	Set Avg ← Avg + MImg(x, y)
	Set Count ← Count + 1
	End If
	End For
	If Count = 0 **Then Set** Count ← 1
	Set Avg ← Avg / Count
	For all r **Do** {Source ≤ r ≤ Destination}
	Set x ← C.x + (r * cos(th*pi/180))
	Set y ← C.y + (r * sin(th*pi/180))
	If x ≥ 0 **And** x ≤ w-1 **And** y ≥ 0 **And** y ≤ h-1 **Then**
	If r < BAe - R_p **Then**
	If MImg(x,y) ≤ Avg **Or** r < BBs - R_p **Then**
	Set V(i, j) ← 0
	Else
	Set V(i, j) ← 1
	End If
	Else
	Set V(i, j) ← 1
	End If
	Else
	Set V(i, j) ← 1
	End If
	Set j ← j + 1
	End For
	Set j ← 0, i ← i + 1
	End For
	For all i, j **Do** {0 ≤ i ≤ 46, 0 ≤ j ≤ L-1}
	If V(i, j) ≠ V(i, j+1) **And** V(i, j) = V(i, j+2) **Then Set** V(i, j+1) ← V(i, j)
	End For
	End	

Algorithm 2-Computing Iris Radius	
Input	V() *'Seeking Vectors* C, R_p *'Pupil Center Point, Radius Respectively* L *'Vector Length*
Output	R_i *'Iris Radius*

Processing	**Define** ZL1(23), ZL2(23)
	Set z1 ← 0, z2 ← 0
	For all i **Do** {0 ≤ i ≤ 45}
	Set k ← 0
	For all j **Do Step -1** {L-1 ≤ j ≤ 0}
	If V(i, j) = 1 **Then Set** k ← k+1 **Else Exit For**
	End For
	Set k ← L – k + 1
	If k > BBs – R_p **And** k < BAe – R_p **Then**
	If i < 23 **Then**
	Set ZL1(z1) ← k
	Set z1 ← z1 + 1
	Else
	Set ZL2(z2) ← k
	Set z2 ← z2 + 1
	End If
	End If
	End For
	Set ZL1 ← **SortAscending**(ZL1)
	Set ZL2 ← **SortAscending**(ZL2)
	Set R_{right} ← ZL1(round(z1/2)+1) + R_p
	Set R_{left} ← ZL2(round(z2/2)+1) + R_p
	Set R_i ← Min(R_{right}, R_{left})
	End

Experimental Results

The proposed method examined on all samples of CASIAv4-Interval dataset, which includes 2639 grayscale samples of resolution 320×240, taken in two sessions form 249 individuals, and distributed over 395 classes. Iris outer boundary localization accuracy was 100% by choosing median value of vectors sets, while the mean and most frequent values are gave localization accuracy equal to 98.4% and 99.2% respectively. The optimal values of annual overlapped regions coefficients β_{As}, β_{Bs}, β_{Ae} and β_{Be} was 0, 90, 125 and 135 respectively. Table -1 lists a comparison of proposed method with other researchers' methods who tested CASIAv4-Interval dataset to obtain their results, and Figure-4 shows some of our proposed method result examples.

Table 1– Compassion of proposed method with other researchers' methods.

Researcher	Outer Boundary Accuracy
A. A. Jarjes et al [10]	96.88%
L. Ling and D. de Brito [8]	97%
R. Gupta and A. Kumar [13]	98.72%
M. Mahlouji and A. Noruzi [11]	99.19%
A. Basit et al [12]	99.21%
Proposed	**100%**

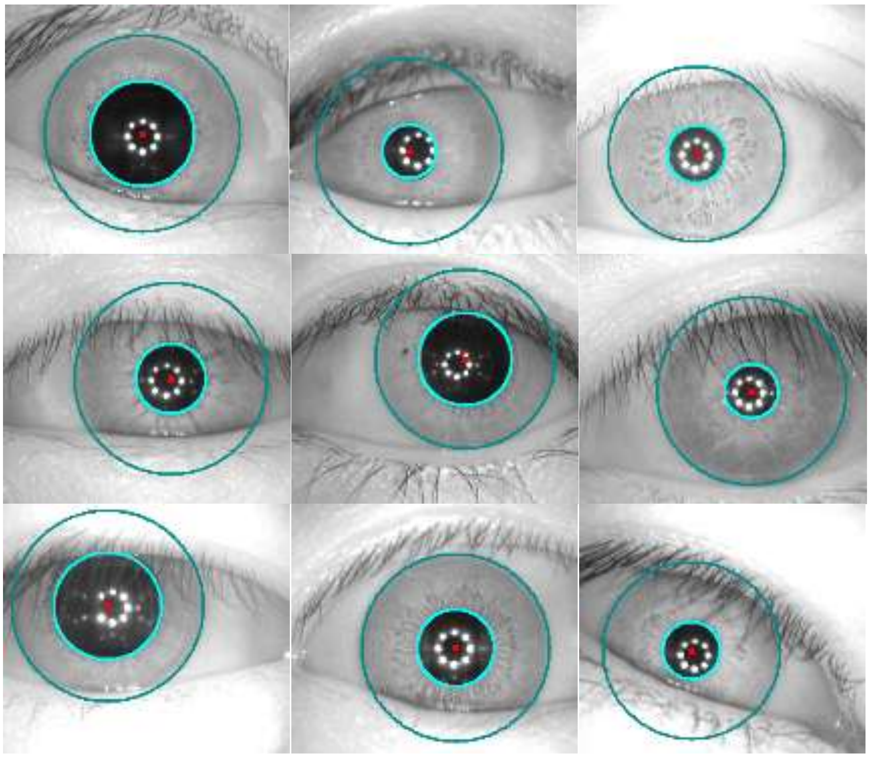

Figure 4– Proposed Method Result Examples

Conclusions

During the experimental attempts, some conclusions are noticed, it is important to talk about. Leading edge technique is an efficient way to isolate foreground from its background, even in hard cases, when the intensity levels of regions are close to each other. In the other hand, the median value is gained the completion against both mean and most frequent values, because the they are affected frequently by incorrect lengths of vectors caused by very closer intensities or the occlusion of eyelids. While the median value is not affected, since it chooses the accurate length independently.

References

1. Adegoke, B.O., Omidiora, E.O., Falohun, S.A. and Ojo, J.A., **2013**. Iris Segmentation: a survey. *International Journal of Modern Engineering Research (IJMER)*, **3**(4): 1885-1889.
2. Liu, C.C., Chung, P.C., Lyu, C.M., Liu, J. and Yu, S.S., **2014**. A novel iris segmentation scheme. *Mathematical Problems in Engineering*, Hindawi Publishing Corporation, Article ID 684212, 2014 (2014), p.14.
3. Cui, J., Wang, Y., Tan, T., Ma, L. and Sun, Z., **2004**, August. A fast and robust iris localization method based on texture segmentation. In Defense and Security Conference (pp. 401-408). International Society for Optics and Photonics.
4. Annapoorani, G., Krishnamoorthi, R., Jeya, P.G. and Petchiammal, S., **2010**. Accurate and Fast Iris Segmentation. *International Journal of Engineering Science and Technology*, **2**(6): 1492-1499.
5. Lefohn, A., Budge, B., Shirley, P., Caruso, R. and Reinhard, E., **2003**. An ocularist's approach to human iris synthesis. *IEEE Computer Graphics and Applications*, **23**(6): 70-75.
6. Daugman, J.G., **1993**. High confidence visual recognition of persons by a test of statistical independence. *IEEE transactions on pattern analysis and machine intelligence*, **15**(11): 1148-1161.
7. Wildes, R.P., **1997**. Iris recognition: an emerging biometric technology. Proceedings of the IEEE, **85**(9): 1348-1363.
8. Ling, L.L. and de Brito, D.F., **2010**. Fast and efficient iris image segmentation. *Journal of Medical and Biological Engineering*, **30**(6): 381-391.

9. Mahadeo, N.K., Papliński, A.P. and Ray, S., **2012**, June. Model-based pupil and iris localization. In Neural Networks (IJCNN), The 2012 International Joint Conference (pp. 1427-1433), IEEE.
10. Jarjes, A.A., Wang, K. and Mohammed, G.J., **2011**. A new Iris segmentation method based on improved snake model and angular integral projection. *Research Journal of Applied Sciences, Engineering and Technology*, **3**(6): 558-568.
11. Mahlouji, M., Noruzi, A., **2012**. Human iris segmentation for iris recognition in unconstrained environments. *IJCSI International Journal of Computer Science Issues*, **9**(3): 149-155.
12. Basit, A., Javed, M.Y. and Masood, S., **2008**, October. Non-circular pupil localization in iris images. In Emerging Technologies, 2008. ICET 2008. 4th International Conference on (pp. 228-231). IEEE.
13. Gupta, R. and Kumar, A., **2015**. Performance Evaluation of Proposed Segmentation Framework with Existing Techniques for Noisy Iris Images. *International Journal of Computer Applications*, **114**(1): 1-6.